J. Fluid Mech. (1982), *vol.* 114, *pp.* 331–341
Printed in Great Britain

Instabilities of finite-amplitude gravity waves on water of finite depth

By JOHN W. McLEAN
Fluid Mechanics Department, TRW Defense and Space Systems Group,
Redondo Beach, CA 90278

(Received 23 March 1981)

A study of the instabilities of finite-amplitude periodic gravity waves has extended recent deep-water results to finite depth. Results are presented for three depths, one greater and two less than the depth for stabilization of two-dimensional long-wave perturbations. The results include those instabilities found by perturbation methods as well as some new types of instability.

1. Introduction

It is well known that a periodic wave train on deep water (Stokes wave) is unstable to modulational perturbations (Benjamin & Feir 1967; Zakharov 1968). A two-dimensional analysis of infinitesimal perturbations of the Stokes wave in the arbitrary depth case shows a similar instability, provided that the fluid is not too shallow (Whitham 1967; Benjamin 1967). Analysis in three dimensions based on Whitham's theory (Hayes 1973) and the multiple scaling technique (Zakharov & Kharitonov 1970; Benney & Roskes 1970) indicates the dominant instability of the finite-depth periodic wave train is three-dimensional, and the instabilities persist to arbitrarily shallow depths.

In this paper, we give details of a numerical investigation of the stability of finite-amplitude, finite-depth water waves to infinitesimal three-dimensional perturbations of arbitrary wavelength. The formulation of the problem and method of solution is similar to the study of the infinite-depth case (McLean *et al.* 1981; McLean 1981).

The instabilities found are qualitatively similar to the deep-water case: bands of instability are associated with resonances deduced from the linear dispersion relation. For small to moderate amplitudes, the lowest-order resonance is dominant, and corresponds to the instabilities previously found by perturbation methods. These instabilities have been investigated by Bryant (1978) with a formulation similar to the present study. Since he kept only the quadratic terms in the equations of motion, only the lowest-order resonance was found. Using the full equations, we have found that the instability associated with the next-order resonance dominates for sufficiently steep waves.

Results are presented for three depths and a range of wave steepness up to about 90 % of the limiting wave amplitudes.

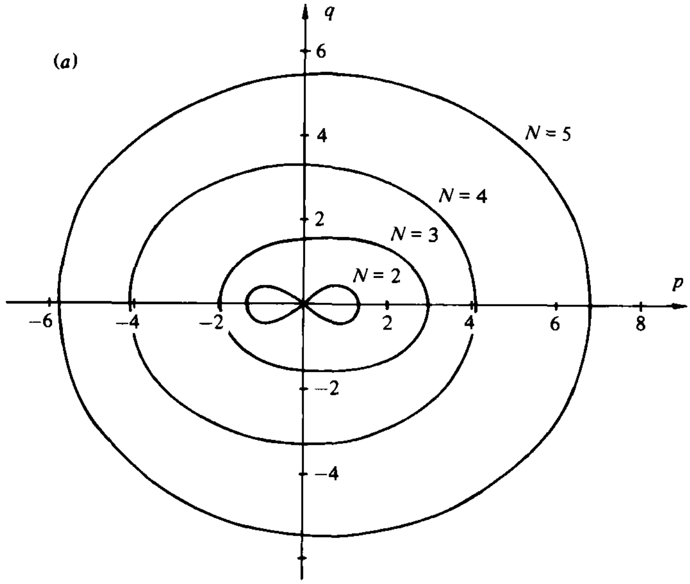

FIGURE 1. Resonance curves from the linear dispersion relation. N is the order of the resonance (equation (11)). (a) $kh = 2{\cdot}0$; (b) $kh = 0{\cdot}5$.

2. Governing equations

The analysis proceeds along the lines of the deep-water case (McLean 1981), with modifications for finite depth. We consider two-dimensional, steadily propagating surface gravity waves of permanent form on an inviscid, irrotational, incompressible fluid of finite depth. In a frame of reference moving with the wave, the governing equations are

$$\left.\begin{aligned} \nabla^2\bar{\phi} &= 0 \quad (-h < z < \bar{\eta}), \\ \bar{\phi}_z &= 0 \quad (z = -h), \end{aligned}\right\} \tag{1}$$

$$\left.\begin{aligned} \bar{\eta} + \tfrac{1}{2}(\bar{\phi}_x^2 + \bar{\phi}_z^2) &= \tfrac{1}{2}B \\ \bar{\phi}_x \bar{\eta}_x - \bar{\phi}_z &= 0 \end{aligned}\right\} \quad (z = \bar{\eta}), \tag{2}$$

where $\bar{\phi}(x, z)$ is the velocity potential, $z = \bar{\eta}(x)$ is the free surface, h is the mean depth, and B is the Bernoulli constant. Without loss of generality, the gravitational acceleration is one and the unperturbed wave has wavelength $\lambda = 2\pi$. These equations admit two-dimensional steady solutions of the form:

$$\left.\begin{aligned} \bar{\eta}(x) &= \sum_{n=1}^{\infty} A_n \cos(nx), \\ \bar{\phi}(x, z) &= -Cx + \sum_{n=1}^{\infty} B_n \sin(nx) \frac{\cosh n(z+h)}{\sinh(nh)}, \end{aligned}\right\} \tag{3}$$

where the Fourier coefficients A_n, B_n and the 'phase speed' C are functions of the wave steepness ka and the Bernoulli constant B (or equivalently the mean depth h), where a is one-half the crest-to-trough height, and k is the wavenumber ($k = 2\pi/\lambda = 1$).

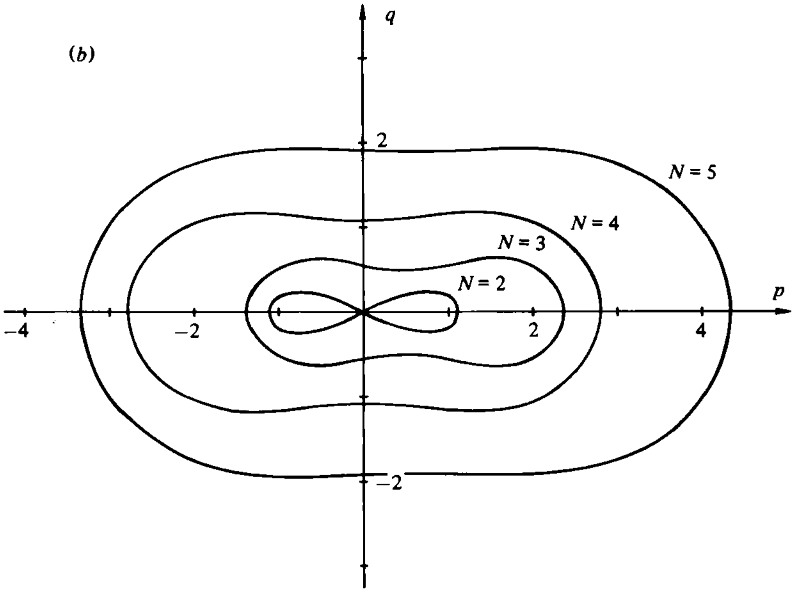

FIGURE 1 (b). For legend see p. 332.

We consider the stability of these two-dimensional steady waves to an infinitesimal three-dimensional disturbance. Let

$$\eta = \bar{\eta} + \eta', \quad \phi = \bar{\phi} + \phi',$$

where the perturbations $\eta'(x,y,t)$, $\phi'(x,y,z,t)$ satisfy $\eta' \ll \bar{\eta}$, $\phi' \ll \bar{\phi}$. In the frame of reference moving with the steady wave, the linearized equations are

$$\left.\begin{aligned} \phi'_t + \eta' + \bar{\phi}_x \phi'_x + \bar{\phi}_z \phi'_z + (\bar{\phi}_x \bar{\phi}_{xz} + \bar{\phi}_z \bar{\phi}_{zz})\, \eta' &= 0, \\ \eta'_t + \bar{\phi}_x \eta'_x + \bar{\eta}_x \phi'_x + (\bar{\phi}_{xz} \bar{\eta}_x - \bar{\phi}_{zz})\, \eta' - \phi'_z &= 0, \end{aligned}\right\} \tag{4}$$

where the equations are to be satisfied on the unperturbed free surface. The normal modes of the disturbance have the form:

$$\left.\begin{aligned} \eta' &= e^{-i\sigma t} e^{i(px+qy)} \sum_{j=-\infty}^{\infty} a_j e^{ijx}, \\ \phi' &= e^{-i\sigma t} e^{i(px+qy)} \sum_{j=-\infty}^{\infty} b_j e^{ijx} \frac{\cosh\,[(p+j)^2+q^2]^{\frac{1}{2}}\,(z+h)}{\sinh\,[(p+j)^2+q^2]^{\frac{1}{2}}\,h}, \end{aligned}\right\} \tag{5}$$

where p and q are arbitrary real numbers. The physical disturbance corresponds to the real part of (5). Substitution of (5) into the linearized equations (4) yields an eigenvalue problem for σ:

$$\left.\begin{aligned} &(1 + \bar{\phi}_x \bar{\phi}_{xz} + \bar{\phi}_z \bar{\phi}_{zz})\, \Sigma a_j e^{ijx} + \Sigma[i(p+j)\,\bar{\phi}_x \cosh k_j(\bar{\eta}+h) \\ &\qquad + \bar{\phi}_z k_j \sinh k_j(\bar{\eta}+h)]\, \frac{b_j e^{ijx}}{\sinh k_j h} = i\sigma \Sigma b_j e^{ijx} \frac{\cosh k_j(\bar{\eta}+h)}{\sinh k_j h}, \\ &\Sigma(\bar{\phi}_{xz}\bar{\eta}_x - \bar{\phi}_{zz} + i(p+j)\,\bar{\phi}_x)\, a_j e^{ijx} + \Sigma[i(p+j)\,\bar{\eta}_x \cosh k_j(\bar{\eta}+h) \\ &\qquad - k_j \sinh k_j(\bar{\eta}+h)]\, \frac{b_j e^{ijx}}{\sinh k_j h} = i\sigma \Sigma a_j e^{ijx}, \end{aligned}\right\} \tag{6}$$

where $k_j = |\mathbf{k}_j| = [(p+j)^2+q^2]^{\frac{1}{2}}$. These equations are to be satisfied for $0 < x < 2\pi$. Instability corresponds to $\mathscr{I}\sigma > 0$.

For $ka = 0$, the eigenvalues and corresponding eigenfunctions of (6) are:

$$\left.\begin{aligned} \eta'_n &= e^{-i\sigma_n t} e^{i[(p+n)x+qy]}, \\ \sigma_n &= -C(p+n) \pm [k \tanh (kh)]^{\frac{1}{2}} \end{aligned}\right\} \tag{7}$$

where $C = (\tanh h)^{\frac{1}{2}}$. Nonlinear effects ($ka > 0$) can lead to instability if these eigenvalues agree for different n and the same p and q in the linear approximation:

$$\sigma^{\pm}_{n_1}(p,q) = \sigma^{\pm}_{n_2}(p,q) \tag{8}$$

for some $[n_1, n_2]$ and choice of the propagation sense. As in the deep-water case, the solution to (8) can be divided into two classes:

Class I,

$$\left.\begin{aligned} \mathbf{k}_1 = (p+m,q), \quad \mathbf{k}_2 = (p-m,q), \\ \sigma^{+}_{m}(p,q) = \sigma^{-}_{-m}(p,q), \\ [k_1 \tanh (k_1 h)]^{\frac{1}{2}} + [k_2 \tanh (k_2 h)]^{\frac{1}{2}} = 2mC; \end{aligned}\right\} \tag{9}$$

Class II,

$$\left.\begin{aligned} \mathbf{k}_1 = (p+m,q), \quad \mathbf{k}_2 = (p-m-1,q) \\ \sigma^{+}_{m}(p,q) = \sigma^{-}_{-m-1}(p,q) \\ [k_1 \tanh (k_1 h)]^{\frac{1}{2}} + [k_2 \tanh (k_2 h)]^{\frac{1}{2}} = (2m+1)\,C. \end{aligned}\right\} \tag{10}$$

Here m is a positive integer. Class I curves are symmetric about $p = 0$, $q = 0$, while class II curves are symmetric about $p = \frac{1}{2}$, $q = 0$ (figure 1).

Alternatively, the coincidence of eigenvalues can be interpreted as a resonance of two infinitesimal waves with a 'carrier' wave, for which the resonance condition is

$$w_1 = -w_2 + Nw_0, \quad \mathbf{k}_1 = \mathbf{k}_2 + N\mathbf{k}_0, \tag{11}$$

where $\mathbf{k}_0 = (1,0)$, $\mathbf{k}_1 = (p+N,q)$, $\mathbf{k}_2 = (p,q)$ and $w_i = [k_i \tanh (k_i h)]^{\frac{1}{2}}$. Class I, $m = 1$ corresponds to $N = 2$; class II, $m = 1$ corresponds to $N = 3$. For deep water, McLean *et al.* 1981 (see also McLean 1981) demonstrated that these resonances produce instability bands for finite amplitude.

3. Numerical treatment

The computations consist of two parts, calculation of the unperturbed wave $\bar{\eta}$, $\bar{\phi}$ and subsequent solution of the eigenvalue problem. To calculate the unperturbed wave, it proved convenient to solve for x and z as functions of the velocity potential ϕ and stream function ψ. In these variables, the unperturbed flow can be expressed as:

$$\left.\begin{aligned} x(\phi,\psi) &= \frac{\phi}{C} + \sum_{n=1}^{\infty} \frac{H_n}{n} \frac{\cosh n(\psi-\psi_0)/C}{\sinh(-n\psi_0/C)} \sin \frac{n\phi}{C}, \\ z(\phi,\psi) &= \frac{\psi}{C} + \frac{H_0}{2} + \sum_{n=1}^{\infty} \frac{H_n}{n} \frac{\sinh n(\psi-\psi_0)/C}{\sinh(-n\psi_0/C)} \cos \frac{n\phi}{C}. \end{aligned}\right\} \tag{12}$$

The bottom is the streamline $\psi = \psi_0$, and the free surface is $\psi = 0$. The free surface boundary condition may be expressed as (Longuet-Higgins 1978):

$$\int_0^{2\pi C} e^{im(\phi/C)} z[x_\phi + i\gamma_m z_\phi]|_{\psi=0} \, d\phi = 0 \quad (m = 1, 2, 3, \ldots), \tag{13}$$

$$\langle \eta \rangle \equiv \frac{1}{2\pi}\int_0^{2\pi} \eta(x)\,dx = \frac{1}{2\pi}\int_0^{2\pi C} z(\phi, 0)\, x_\phi(\phi, 0)\, d\phi$$
$$= -\frac{1}{4\pi}\int_0^{2\pi C} \frac{d\phi}{x_\phi(\phi, \psi_0)}, \tag{14}$$

where $\gamma_m = \coth(-m\psi_0/C)$. Substitution of (12) into (13) and (14) yields:

$$2\frac{H_m}{m} + 2H_0 H_m \gamma_m + \sum_{n=1}^{\infty} \frac{H_n H_{n+m}}{n+m}(\gamma_n - \gamma_m) + \sum_{n=1}^{\infty} \frac{H_n H_{n+m}}{n}(\gamma_{n+m} + \gamma_m)$$
$$+ \sum_{n=1}^{m-1} \frac{H_n H_{m-n}}{n}(\gamma_{m-n} + \gamma_m) = 0 \quad (m = 1, 2, 3, \ldots), \tag{15}$$

$$\frac{1}{2}\left(H_0 + \sum_{n=1}^{\infty} \frac{H_n^2 \gamma_n}{n}\right) = -\frac{1}{4\pi}\int_0^{2\pi C} \frac{d\phi}{x_\phi(\phi, \psi_0)}. \tag{16}$$

The mean depth is given by

$$\langle \eta \rangle - z(\phi, \psi_0) = -\frac{\psi_0}{C} + \frac{1}{2}\sum_{n=1}^{\infty} \frac{H_n^2 \gamma_n}{n}. \tag{17}$$

Equations (15) are quadratic in the unknowns H_n as in the deep-water case. The right-hand side of (16) introduces a more complicated nonlinear term for finite depth. The nonlinear system constructed from (15), (16), and an equation specifying the wave amplitude is truncated at L Fourier modes and solved by Newton's method. The contribution to the Jacobian from the right-hand side of (16) is

$$\frac{\delta}{\delta H_n}\left\{-\frac{1}{4\pi}\int_0^{2\pi C} \frac{d\phi}{x_\phi}\right\} = \frac{1}{4\pi C}\frac{1}{\sinh(-n\psi_0/C)}\int_0^{2\pi C} \frac{\cos(n\phi/C)}{x_\phi^2}\, d\phi. \tag{18}$$

Since the integrands of these terms are periodic, they may be evaluated accurately using the trapezoidal rule (Isaacson & Keller 1966). The truncation L is chosen so the last coefficient is sufficiently small (10^{-12} for most runs). The truncation was varied between 50 and 350 depending on the wave steepness. Twenty-five points were generally adequate to evaluate the integrals in (16) and (18).

To compute the steady wave, we fix the unperturbed fluid depth $d = -\psi_0/C$. This represents the depth of a uniform stream moving with velocity C which has the same mass flux as the steady wave. For a given d, the wave is computed over a range of wave amplitudes up to about 90 % of the limiting wave steepness (as given by Cokelet 1977). The computational economics of performing Newton's method on large systems prevents us from continuing to steeper waves, which require more than 350 Fourier modes to describe the wave adequately. The present computations agree with previously published results. The decision to use d rather than the mean depth h was motivated by ease of computation and to allow comparison with Cokelet, who used the same parameter. Variations of h with ka for fixed d do not amount to more than a few per cent for our computation, see table 1.

$d = 2{\cdot}0$, highest wave: $ka = 0{\cdot}425$

			Unperturbed wave		Class I instability				Class II instability			
ka	L	M	C^2	⟨dep⟩	p	q	$\mathscr{R}\sigma$	$\mathscr{I}\sigma$	p	q	$\mathscr{R}\sigma$	$\mathscr{I}\sigma$
0·10	50	6	0·974883	2·005125	0·21	0·15	0·0877	$3{\cdot}19 \times 10^{-3}$	0·5	1·54	0·0	$7{\cdot}24 \times 10^{-4}$
0·20	50	8	1·008101	2·019723	0·31	0·17	0·1220	$1{\cdot}13 \times 10^{-2}$	0·5	1·43	0·0	$6{\cdot}34 \times 10^{-3}$
0·30	100	12	1·065604	2·041079	0·40	0·14	0·1342	$2{\cdot}39 \times 10^{-2}$	0·5	1·21	0·0	$2{\cdot}65 \times 10^{-2}$
0·35	200	20	1·104017	2·052335	0·46	0·08	0·1268	$3{\cdot}31 \times 10^{-2}$	0·5	0·99	0·0	$5{\cdot}23 \times 10^{-2}$
0·39	300	35	1·137932	2·059619	0·62	0·00	0·1055	$4{\cdot}60 \times 10^{-2}$	0·5	0·68	0·0	$1{\cdot}01 \times 10^{-1}$

$d = 1{\cdot}0$, highest wave: $ka = 0{\cdot}325$

			Unperturbed wave		Class I instability				Class II instability			
ka	L	M	C^2	⟨dep⟩	p	q	$\mathscr{R}\sigma$	$\mathscr{I}\sigma$	p	q	$\mathscr{R}\sigma$	$\mathscr{I}\sigma$
0·10	50	6	0·781727	1·006339	0·28	0·19	0·0618	$2{\cdot}34 \times 10^{-3}$	0·5	0·99	0·0	$2{\cdot}04 \times 10^{-3}$
0·20	100	12	0·839925	1·022771	0·42	0·24	0·0964	$9{\cdot}54 \times 10^{-3}$	0·5	0·90	0·0	$1{\cdot}80 \times 10^{-2}$
0·29	300	35	0·919308	1·038987	0·55	0·19	0·0888	$3{\cdot}07 \times 10^{-2}$	0·5	0·62	0·0	$7{\cdot}60 \times 10^{-2}$

$d = 0{\cdot}5$, highest wave: $ka = 0{\cdot}186$

			Unperturbed wave		Class I instability				Class II instability			
ka	L	M	C^2	⟨dep⟩	p	q	$\mathscr{R}\sigma$	$\mathscr{I}\sigma$	p	q	$\mathscr{R}\sigma$	$\mathscr{I}\sigma$
0·10	100	15	0·531461	0·508233	1·16	0·00	0·2273	$4{\cdot}44 \times 10^{-3}$	0·5	0·55	0·0	$8{\cdot}77 \times 10^{-3}$
0·16	300	35	0·599622	0·515655	0·57	0·23	0·0763	$1{\cdot}45 \times 10^{-2}$	0·5	0·50	0·0	$3{\cdot}76 \times 10^{-2}$

TABLE 1. Maximum growth rate as a function of wave steepness; ⟨dep⟩ is the mean depth.

Once the unperturbed wave has been calculated, we return to Cartesian co-ordinates to construct the eigenvalue problem. The perturbations (5) are truncated at M Fourier modes, and the unknown coefficients $\{a_j, b_j\}$ are chosen to satisfy (6) at $2M+1$ points, spaced in equal arclength increments between adjacent crests of the unperturbed wave. The coefficients of (6) are computed from (12) by a straightforward change of variables. The resulting system of order $4M+2$ is of the form:

$$(\mathbf{A} - \sigma \mathbf{B})\,\mathbf{u} = 0, \tag{19}$$

where $\mathbf{u} = \{a_{-M} \ldots a_M, b_{-M} \ldots b_M\}$, and the matrices $\mathbf{A}$ and $\mathbf{B}$ are complex functions of p, q, and the unperturbed wave (which is a function of ka and d). The eigenvalues σ are obtained from a standard eigenvalue solver (QZ algorithm). The truncation M is increased until the relevant eigenvalues have converged. Computations were performed in double precision (14 digits) on a Prime 750 minicomputer. For more details, see McLean (1981).

4. Results

It is well known that weakly nonlinear water waves are unstable or stable to two-dimensional infinitesimal perturbations if the depth kh is greater or less than 1·363 (Whitham 1967). For our numerical study, we have chosen three depths, one greater and two less than this value. The results are presented in figures 2, 3 and 4 and table 1. We first discuss the lowest-order instability.

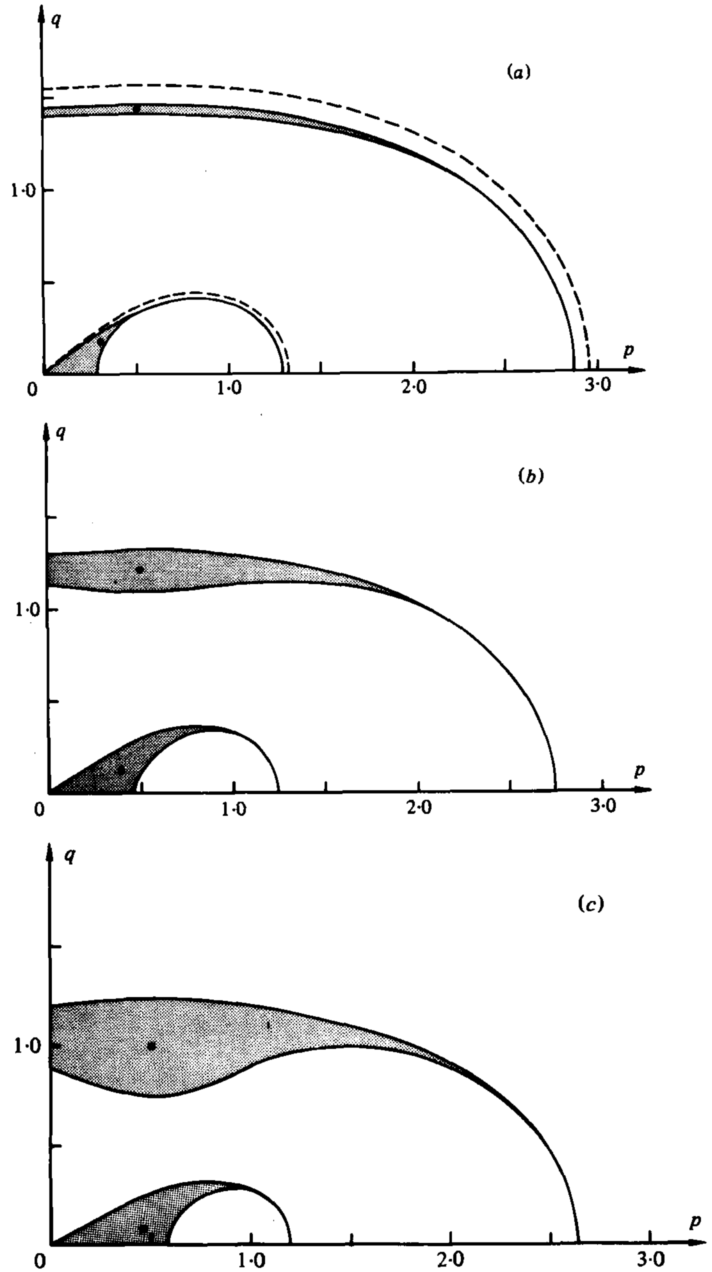

FIGURE 2. Bands of instability for $d = 2 \cdot 0$. The ● labels the point of maximum instability. (*a*) $ka = 0 \cdot 20$, the dashed line is the resonance curve from the linear dispersion relation; (*b*) $ka = 0 \cdot 30$; (*c*) $ka = 0 \cdot 35$; (*d*) $ka = 0 \cdot 39$.

For $d = 2 \cdot 0$, the behaviour of the lowest-order instability ($N = 2$) is very similar to the deep-water case: for small ka, the steady wave is unstable to long-wavelength perturbations which have a growth rate $O(ka)^2$. Note however that the dominant instability at this depth is three-dimensional for small ka. For steeper waves, the long-wavelength perturbations restabilize, and the most unstable wavenumber is

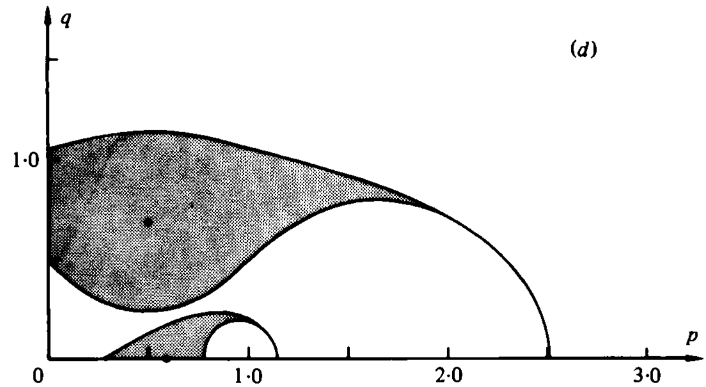

FIGURE 2d. For legend see p. 337.

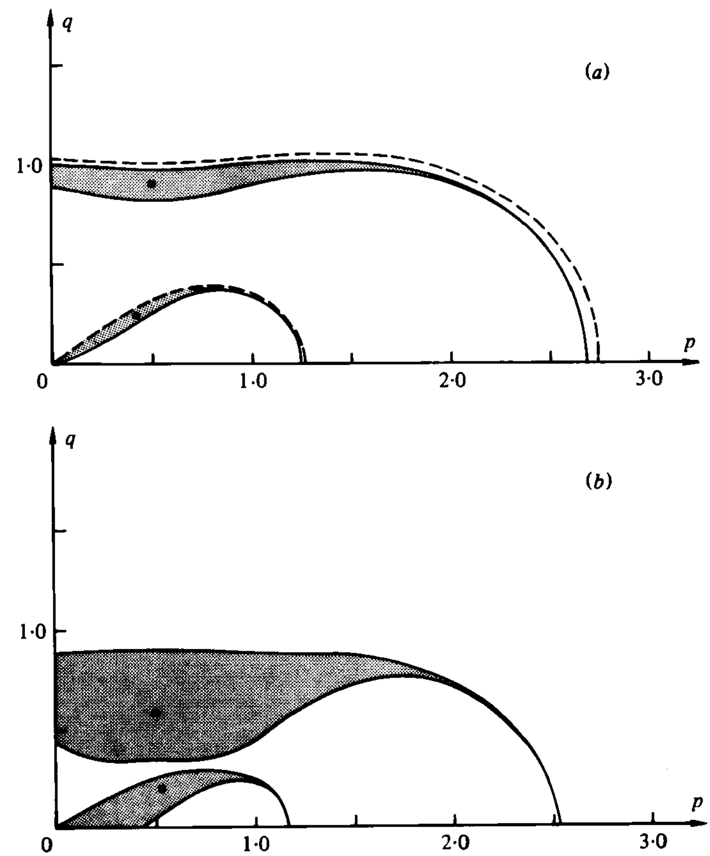

FIGURE 3. Bands of instability for $d = 1{\cdot}0$. (a) $ka = 0{\cdot}20$; (b) $ka = 0{\cdot}29$.

two-dimensional. For the range of amplitudes considered here, this lowest-order instability did not completely restabilize as it does in deep water.

For $d = 1{\cdot}0$, the unperturbed wave is stable to long-wavelength, two-dimensional perturbations for small amplitude, as predicted by Whitham. However, the wave is unstable to three-dimensional perturbations. The growth rate of the unstable side-

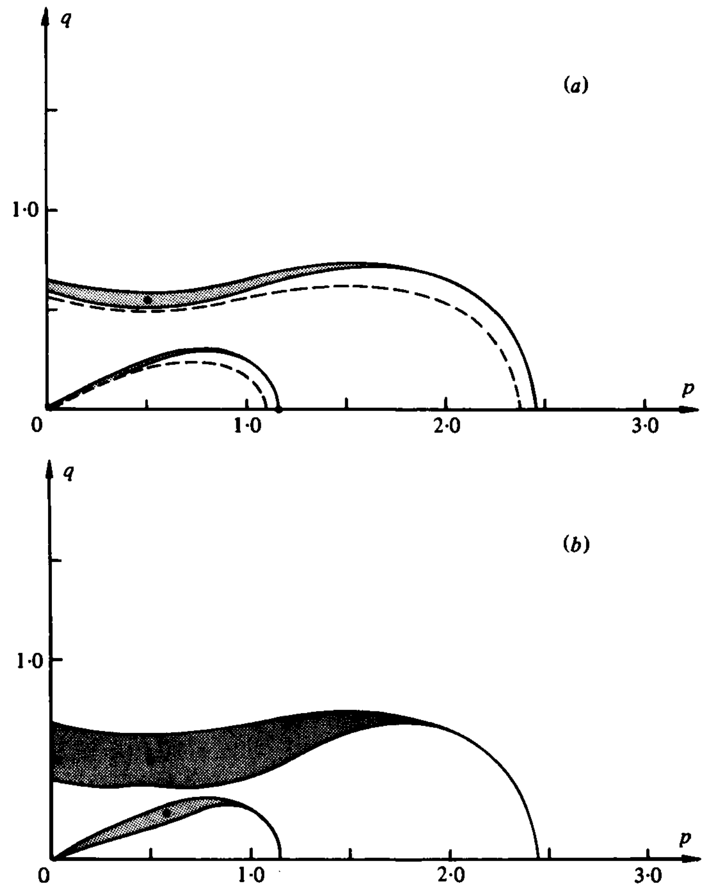

FIGURE 4. Bands of instability for $d = 0{\cdot}5$. (*a*) $ka = 0{\cdot}10$; (*b*) $ka = 0{\cdot}16$.

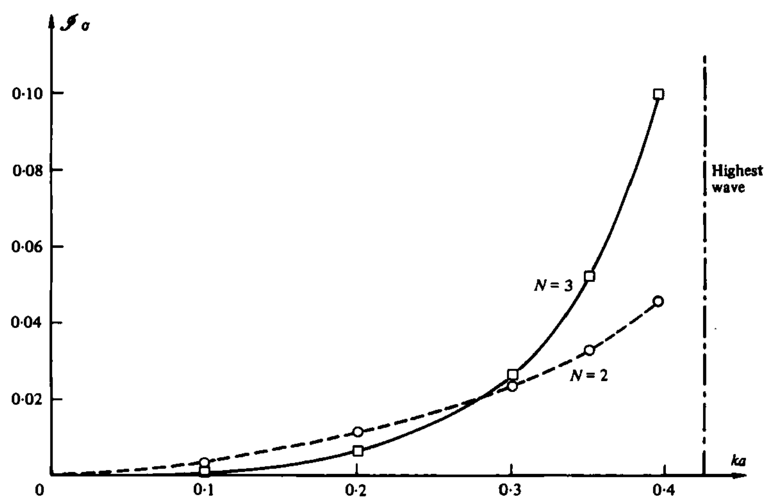

FIGURE 5. Maximum growth rate versus wave steepness for $d = 2{\cdot}0$.

bands is $O(ka)^2$. For $ka = 0{\cdot}29$, two-dimensional perturbations are found to be unstable, although they are dominated by three-dimensional instabilities.

The shallowest case we have considered, $d = 0{\cdot}5$, is most unstable (at least for small ka) to a two-dimensional perturbation with a length scale comparable to the length scale of the unperturbed wave, in contrast to the familiar two-dimensional long-wave perturbations which are the dominant instabilities in deep water. Two-dimensional long-wave perturbations are stable at this depth. For larger amplitudes, three-dimensional instabilities again dominate.

The next-order resonance ($N = 3$) is completely analogous to the deep-water case: the maximum growth rate occurs for $p = \frac{1}{2}$, $q \neq 0$ and has $\mathscr{I}\sigma = O(ka)^3$, $\mathscr{R}\sigma = 0$. Thus the dominant instability propagates with the unperturbed wave with twice the spatial period. The stability boundary at $p = \frac{1}{2}$ is a point of neutral stability ($\sigma = 0$), and suggests a bifurcation into a steady three-dimensional wave pattern (see Saffman & Yuen 1980 for a discussion of deep-water bifurcation). While this third-order resonance is initially weaker than the second-order resonance, it becomes dominant for sufficiently steep waves, see figure 5 and table 1.

In the deep-water case it has been verified that the Nth-order resonance leads to an instability with growth rate $(ka)^N$ for $N = 2, 3, 4, 5$. We expect this to be true for finite depth, and have verified this for $N = 2$ and 3.

5. Discussion

We have presented the results of a numerical study of the stability of steady periodic gravity waves for three depths. The results are similar to the deep-water case, but there are some interesting differences, particularly in the case of the lowest-order resonance. In deep water, this resonance leads to an instability with growth rate of order $(ka)^2$, for which the most unstable perturbation is two-dimensional. For finite depth, the present examples show the shift to a three-dimensional perturbation, in agreement with perturbation analysis (Benney & Roskes 1970). We have also demonstrated the stabilization of two-dimensional long-wave perturbations for $kh < 1{\cdot}363$ as predicted by Whitham (1967).

For deep water, the tip of the lobe of the resonance curve ($p = \frac{5}{4}$, $q = 0$), has been shown to lead to an instability of order $(ka)^4$ (McLean 1981). For finite depth, the corresponding point for $q = 0$, p satisfying

$$[|1+p|\tanh|1+p|h]^{\frac{1}{2}} + [|1-p|\tanh|1-p|h]^{\frac{1}{2}} = 2[\tanh h]^{\frac{1}{2}}, \qquad (20)$$

is observed to have a growth rate $O(ka)^2$, and is initially the dominant instability for $kh = 0{\cdot}5$. This instability has not been obtained by perturbation methods, which have considered the case $p \ll 1$, $q \ll 1$.

The instability associated with the next-order resonance is qualitatively similar to the deep-water case. In deep water, it has been shown that, for $ka > 0{\cdot}406$, the instability band touches the p-axis at $p = \frac{1}{2}$, resulting in an unstable two-dimensional subharmonic perturbation. Although for finite depth, the stability band approaches the p-axis with increasing ka, the band does not reach the axis for the wave amplitudes considered here. In light of the present calculations, it seems unlikely that the band will touch the axis for steeper waves in the two shallower cases.

REFERENCES

BENJAMIN, T. B. 1967 Instability of periodic wavetrains in nonlinear dispersive systems. *Proc. Roy. Soc.* A **299**, 59–75.

BENJAMIN, T. B. & FEIR, J. E. 1967 The disintegration of wavetrains on deep water. *J. Fluid Mech.* **27**, 417–430.

BENNEY, D. J. & ROSKES, G. J. 1970 Wave instabilities. *Studies Appl. Math.* **48**, 377–385.

BRYANT, P. J. 1978 Oblique instability of periodic waves in shallow water. *J. Fluid Mech.* **86**, 783–792.

COKELET, E. D. 1977 Steep gravity waves in water of arbitrary uniform depth. *Proc. Roy. Soc.* A **286**, 184–230.

HAYES, W. D. 1973 Group velocity and nonlinear dispersive wave propagation. *Proc. Roy. Soc.* A **332**, 199–221.

ISAACSON, E. & KELLER, H. B. 1966 *Analysis of Numerical Methods*, pp. 340–341. John Wiley & Sons.

LONGUET-HIGGINS, M. S. 1978 Some new relations between Stokes coefficients in the theory of gravity waves. *J. Inst. Math. Applics.* **22**, 261–273.

MCLEAN, J. W. 1981 Instabilities of finite amplitude water waves. *J. Fluid Mech.* **114**, 315–330.

MCLEAN, J. W., MA, Y. C., MARTIN, D. U., SAFFMAN, P. G. & YUEN, H. C. 1981 Three dimensional instability of finite amplitude water waves. *Phys. Rev. Letters*, **46**, 817–820.

SAFFMAN, P. G. & YUEN, H. C. 1980 A new type of three-dimensional deep-water wave of permanent form. *J. Fluid Mech.* **101**, 797–808.

WHITHAM, G. B. 1967 Non-linear dispersion of water waves. *J. Fluid Mech.* **27**, 399–412.

ZAKHAROV, V. E. 1968 Stability of periodic waves of finite amplitude on the surface of a deep fluid. *J. Appl. Mech. Tech. Phys.* **2**, 190–194.

ZAKHAROV, V. E. & KHARITONOV, V. G. 1970 Instability of monochromatic waves on the surface of a liquid of arbitrary depth. *J. Appl. Mech. Tech. Phys.* **11**, 747–751.